LETTER

doi:10.1038/nature13980

Piezo2 is the major transducer of mechanical forces for touch sensation in mice

Sanjeev S. Ranade[1], Seung-Hyun Woo[1], Adrienne E. Dubin[1], Rabih A. Moshourab[2,3], Christiane Wetzel[2], Matt Petrus[4], Jayanti Mathur[4], Valérie Bégay[2], Bertrand Coste[1]†, James Mainquist[4], A. J. Wilson[4], Allain G. Francisco[1], Kritika Reddy[1], Zhaozhu Qiu[1,4], John N. Wood[5], Gary R. Lewin[2] & Ardem Patapoutian[1]

The sense of touch provides critical information about our physical environment by transforming mechanical energy into electrical signals[1]. It is postulated that mechanically activated cation channels initiate touch sensation, but the identity of these molecules in mammals has been elusive[2]. Piezo2 is a rapidly adapting, mechanically activated ion channel expressed in a subset of sensory neurons of the dorsal root ganglion and in cutaneous mechanoreceptors known as Merkel-cell–neurite complexes[3,4]. It has been demonstrated that Merkel cells have a role in vertebrate mechanosensation using Piezo2, particularly in shaping the type of current sent by the innervating sensory neuron[4–6]; however, major aspects of touch sensation remain intact without Merkel cell activity[4,7]. Here we show that mice lacking Piezo2 in both adult sensory neurons and Merkel cells exhibit a profound loss of touch sensation. We precisely localize Piezo2 to the peripheral endings of a broad range of low-threshold mechanoreceptors that innervate both hairy and glabrous skin. Most rapidly adapting, mechanically activated currents in dorsal root ganglion neuronal cultures are absent in *Piezo2* conditional knockout mice, and *ex vivo* skin nerve preparation studies show that the mechanosensitivity of low-threshold mechanoreceptors strongly depends on Piezo2. This cellular phenotype correlates with an unprecedented behavioural phenotype: an almost complete deficit in light-touch sensation in multiple behavioural assays, without affecting other somatosensory functions. Our results highlight that a single ion channel that displays rapidly adapting, mechanically activated currents *in vitro* is responsible for the mechanosensitivity of most low-threshold mechanoreceptor subtypes involved in innocuous touch sensation. Notably, we find that touch and pain sensation are separable, suggesting that as-yet-unknown mechanically activated ion channel(s) must account for noxious (painful) mechanosensation.

Dorsal root ganglion (DRG) neurons have pseudounipolar axons that terminate in the skin where they form specialized mechanoreceptors that are tuned to detect mechanical forces such as stretch, indentation and vibration[1]. A diverse set of low-threshold mechanoreceptors (LTMRs) are distributed within hairy and glabrous skin. Lanceolate and circumferential endings that contain a mixed population of Aβ, Aδ and C LTMRs are specific to hairy skin, whereas various corpuscles that consist of rapidly adapting Aβ LTMRs are unique to glabrous skin[1,8]. Merkel-cell–neurite complexes that mediate slowly adapting responses in Aβ fibres are present in both skin types[4]. Together, these structurally diverse LTMRs detect mechanical stimuli relevant to innocuous touch sensation.

We had previously shown that Piezo2 was expressed in Merkel-cell–neurite complexes and that Merkel cells partly contributed to slowly adapting type I firing[4,5,9]. Whether Piezo2 was also expressed in other cutaneous mechanoreceptors and whether it functioned as the primary mechanotransduction ion channel was not known. We therefore used a recently generated mouse line, *Piezo2-GFP*, where green fluorescent protein (GFP) was fused to the carboxy terminus of *Piezo2*, to detect localization of Piezo2 at the site of mechanical transduction: in the nerve terminals of sensory neurons that project to the skin[4]. In hairy skin, GFP expression was found in both lanceolate endings and circumferential fibres that have varying degrees of myelination and wrap around the bulge region of hair follicles (Fig. 1a, b). Consistent with our previous analysis, Piezo2 was expressed in Merkel cells in both hairy and glabrous skin (Fig. 1c)[4,5]. In glabrous skin, Piezo2 was also expressed in Meissner's corpuscles (Fig. 1d). Overall, Piezo2 expression is found in a broad range of LTMRs that sense mechanical stimuli relevant to touch sensation.

Constitutive deletion of Piezo2 led to perinatal lethality; therefore, we used an inducible strategy to delete Piezo2 in adult mice[10]. The *Advil-creERT2* mouse line allowed for tamoxifen-induced activation of Cre recombinase under the advillin promoter in sensory neurons and in epidermal Merkel cells[11]. We first characterized the expression overlap in DRGs between *Advil-creERT2* and Piezo2 by mating the *Advil-creERT2* mouse to the Ai9 tdTomato reporter line. In agreement with a previous report, we found that 87% of DRG neurons express tdTomato (766 of 876 total cells) (Fig. 2a). Co-expression analysis of tdTomato epifluorescence with anti-Piezo2 antibody staining showed that 82% of Piezo2$^+$ cells were also tdTomato$^+$ (343 of 419 cells out of 876 total) (Fig. 2a)[4]. We also detected expression of tdTomato in epidermal Merkel cells (data not shown), indicating the *Advil-creERT2* mouse line would lead to deletion of Piezo2 in all cell types either proposed or known to be relevant to somatosensory transduction[11]. These data further indicated that while *Advil-creERT2* would ablate Piezo2 in most DRG neurons, a small number of Piezo2$^+$/Cre$^-$ neurons might still remain intact. We then mated the *Advil-creERT2* mouse to a previously generated conditional knockout (CKO) mouse line, *Piezo2*^{fl}, and found that Piezo2 expression levels were similar between genotypes before tamoxifen injections (Fig. 2b, top). After tamoxifen injections, Piezo2 immunostaining in *Piezo2*^{CKO} mice showed a marked decrease in the number of Piezo2-positive DRG neurons compared to wild-type (*Piezo2*^{WT}) mice (Fig. 2b, bottom) and quantitative real-time PCR (qPCR) analysis revealed a ~90% deletion of overall *Piezo2* transcripts in isolated DRG neurons (Fig. 2c).

Previous reports had shown that cultured DRG neurons that were transfected with small interfering RNA (siRNA) for *Piezo2* showed a selective decrease in rapidly adapting, mechanically activated currents[3,12]. We determined the sensitivity of cultured DRG neurons from *Piezo2*^{CKO} mice to mechanical indentation using a piezoelectrically actuated blunt glass probe[10,13,14]. DRGs from *Piezo2*^{CKO} mice had dramatically fewer neurons with rapidly adapting whole-cell current responses compared to controls (Fig. 2d and Extended Data Fig. 1a), and a corresponding increase in the proportion of mechanically insensitive neurons. There were no significant effects on intermediately adapting and slowly adapting currents (Fig. 2d and Extended Data Fig. 1b, c), and there were no differences between genotypes for access resistance, membrane resistance

[1]Howard Hughes Medical Institute, Molecular and Cellular Neuroscience, Dorris Neuroscience Center, The Scripps Research Institute, La Jolla, California 92037, USA. [2]Department of Neuroscience, Max-Delbrück Center for Molecular Medicine, Robert-Rössle Straße 10, D-13092 Berlin, Germany. [3]Klinik für Anästhesiologie mit Schwerpunkt Operative Intensivmedizin, Campus Charité Mitte and Virchow-Klinikum Charité, Universitätsmedizin Berlin, Augustburgerplatz 1, 13353 Berlin, Germany. [4]Genomics Institute of the Novartis Research Foundation, San Diego, California 92121, USA. [5]Molecular Nociception Group, Wolfson Institute for Biomedical Research, University College London, London WC1E 6BT, UK. †Present address: Ion Channels and Sensory Transduction group, Aix Marseille University, CNRS, CRN2M-UMR 7286, 13344 Marseille, France.

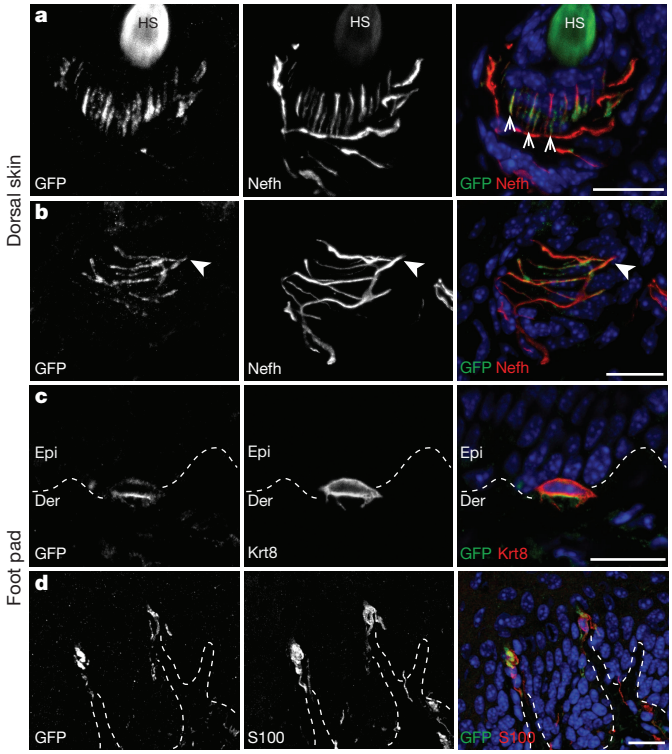

Figure 1 | Piezo2 is localized at the nerve terminals of sensory neurons that innervate the skin. **a**, **b**, Representative images of immunostaining of GFP, Nefh and DAPI (4′,6-diamidino-2-phenylindole, blue) in the hair follicle of dorsal skin of *Piezo2-GFP* mice. GFP staining indicates localization of the Piezo2–GFP fusion protein and Nefh marks myelinated neurons. **c**, Representative image of immunostaining of GFP, Krt8 (a specific marker of Merkel cells) and DAPI (blue) in glabrous skin of *Piezo2-GFP* mice. **d**, Representative images of immunostaining of GFP and S100 (a marker of Schwann cells) in glabrous skin. Arrows mark lanceolate endings (**a**) and arrowheads mark circumferential fibres (**b**). Dashed lines demarcate the epidermal–dermal junction (**c** and **d**). Der, dermis; Epi, epidermis; HS, hair shaft. Scale bars, 20 μm.

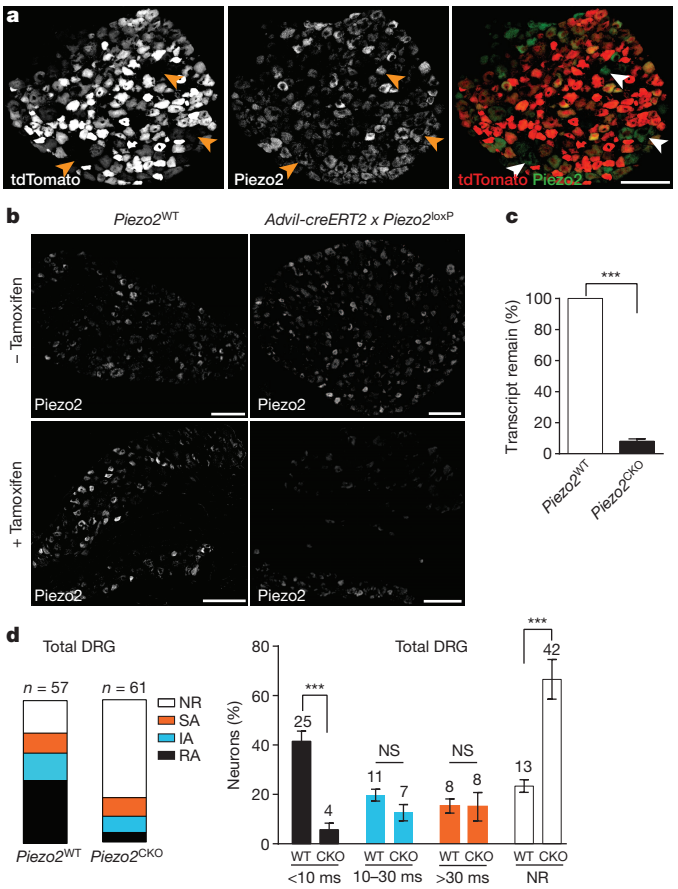

Figure 2 | *Advil-creERT2* mediates efficient deletion of Piezo2 and leads to specific loss of rapidly adapting, mechanically activated currents in cultured DRG neurons. **a**, Immunostaining of DRG neurons from tamoxifen-treated *Advil-creERT2* × Ai9 mice for tdTomato epifluorescence and anti-Piezo2 antibody. Arrowheads indicate the relatively few tdTomato$^-$/Piezo2$^+$ neurons that would presumably not be deleted in *Piezo2*^{CKO} mice. **b**, Representative images of immunostaining using anti-Piezo2 antibody in DRGs from *Advil-creERT2* × *Piezo2*^{loxP} mice before and after tamoxifen treatment. **c**, qPCR of *Piezo2* from isolated DRGs from *Piezo2*^{WT} and *Piezo2*^{CKO} mice with *Piezo2*^{WT} values normalized at 100% ($n = 3$ independent experiments, $P < 0.0001$, Student's *t*-test). **d**, The proportion of DRG neurons responding with rapidly (RA, $\tau_{inact} < 10$ ms), intermediately (IA, τ_{inact} 10–30 ms) and slowly (SA, $\tau_{inact} > 30$ ms) adapting mechanically activated currents from *Piezo2*^{WT} and *Piezo2*^{CKO} littermates. NR, non-responsive to displacements of at least one-third cell diameter; NS, not significant. Results from $n = 3$ independent experiments. Error bars represent s.e.m., $^{***}P < 0.0001$ for rapidly adapting and $^{***}P < 0.0005$ for non-responsive, Student's *t*-test. Scale bars, 100 μm (**a**, **b**).

and resting membrane potential (Extended Data Table 1). Notably, we observed a wide range of low and high apparent thresholds for rapidly adapting currents in *Piezo2*^{WT} neurons, while none of the remaining rapidly adapting responses in *Piezo2*^{CKO} neurons had low apparent thresholds (Extended Data Fig. 2). Whether the rapidly adapting activity in sensory neurons of *Piezo2*^{CKO} mice is mediated by any remaining Piezo2 or another mechanically activated channel is not known. Nonetheless, these results suggest that Piezo2 accounts for the majority of rapidly adapting currents in cultured DRG neurons.

In order to confirm that loss of Piezo2 did not affect the integrity of DRG neurons, we performed immunostaining analyses of DRG neurons using markers of various subpopulations. The expression patterns of neurofilament heavy polypeptide (Nefh), thymidine hydroxylase (TH) and calcitonin gene-related peptide (CGRP) were unaffected in *Piezo2*^{CKO} DRGs relative to *Piezo2*^{WT} DRGs (Extended Data Fig. 3a–f). Moreover, *Piezo2*^{WT} mice, as well as *Piezo2*^{CKO} mice, showed normal cutaneous mechanoreceptor formation including Merkel-cell–neurite complexes (Extended Data Fig. 4a, d), lanceolate and circumferential endings (Extended Data Fig. 4b, e, f), and Meissner's corpuscles (Extended Data Fig. 4c, g). We also performed calcium imaging in cultured DRG neurons and found no significant differences in the number of capsaicin-responsive cells between the two genotypes (data not shown).

Loss of mechanically activated currents in cultured DRG neurons is expected to be associated with a loss of mechanosensitivity of sensory fibres in the skin[15]. We tested this using an *ex vivo* skin nerve preparation in which mechanically insensitive fibres were identified with an electrical search technique (Extended Data Table 2)[15,16]. In *Piezo2*^{CKO} mice, 50% of the Aβ fibres had no detectable mechanosensitivity compared to less than 10% of Aβ fibres from *Piezo2*^{WT} mice (Fig. 3a). There was a non-significant decrease in the proportion of Aδ fibres in *Piezo2*^{CKO} lacking mechanosensitivity, and there was no significant loss of mechanosensitivity in C fibres (<10% in both genotypes) (Fig. 3a). Despite the marked loss of mechanosensitivity, the axonal conduction velocities of Aβ, Aδ and C fibres were unchanged in *Piezo2*^{CKO} mice compared to controls (Extended Data Fig. 5a).

We also investigated Aβ fibres with a mechanosensitive receptive field using a series of ramp and hold force stimuli with ramp phases of different velocities (Fig. 3b, c). Slowly adapting mechanoreceptors associated with Merkel cells are known to have a characteristic irregular firing during static displacement and a prominent dynamic discharge during the ramp[17]. We showed previously that deletion of Piezo2 in Merkel cells led to reduced firing in the static phase but not the dynamic phase[4].

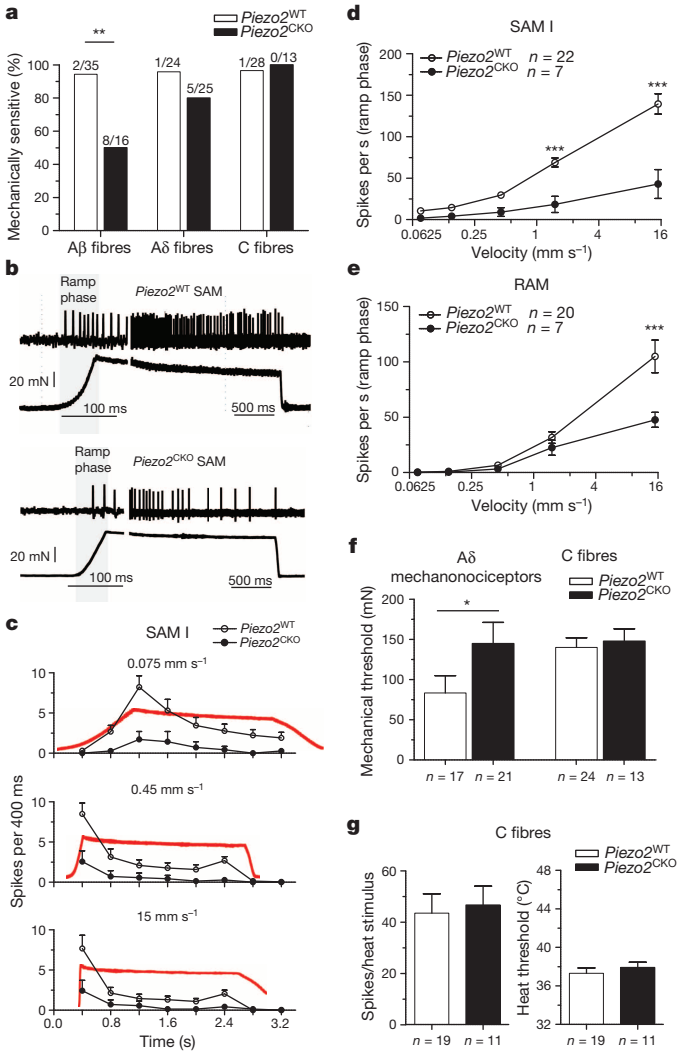

Figure 3 | Piezo2 is required for mechanoreceptor function in *ex vivo* skin nerve preparation. **a**, Proportions of mechanically sensitive Aβ, Aδ and C fibres in *Piezo2*^{CKO} mice compared to *Piezo2*^{WT} controls, one-sided Fisher's exact test, $^{**}P < 0.01$. **b**, Typical examples of SAM I mechanoreceptor responses from *Piezo2*^{CKO} and *Piezo2*^{WT} mice. **c**, Mean discharge rates (400-ms bins) during the course of ramp and hold stimuli with different onset velocities for SAM I receptors. Note the almost complete lack of dynamic ramp discharge in SAM I receptors recorded from *Piezo2*^{CKO} mice. **d**, Normally, SAM I discharge rates increase with increasing ramp speed, however SAM I receptors from *Piezo2*^{CKO} mice showed a strong reduction in velocity sensitivity with firing discharge increasing only marginally with increasing stimulus velocity (repeated measures ANOVA, $F = 19.69$, $P < 0.0001$, with Bonferroni post hoc test, $^{***}P < 0.001$). **e**, Rapidly adapting afferents also displayed reduced velocity sensitivity in *Piezo2*^{CKO} mutant mice (repeated measures ANOVA, $F = 4.36$, $P < 0.05$, with Bonferroni post hoc test, $^{***}P < 0.001$). **f**, Mean force thresholds for nociceptor discharge. Individual nociceptors threshold were calculated by averaging the thresholds of first spikes occurring during the stimulus ramp phase for all six stimuli applied. Note significant elevation of mechanical thresholds for Aδ mechanonociceptors in *Piezo2*^{CKO} mice (Mann–Whitney test, $^{*}P < 0.05$), but no change in C-fibre mechanical thresholds. **g**, Discharge rates and heat thresholds to standard noxious heat ramps did not differ between polymodal C fibres recorded from *Piezo2*^{CKO} and *Piezo2*^{WT} mice. Data are presented as mean ± s.e.m.

Here, most slowly adapting mechanoreceptors encountered in *Piezo2*^{WT} (22 of 31 fibres) and *Piezo2*^{CKO} (7 of 10 fibres) could be classified as probably slowly adapting type I fibres (SAM I) associated with Merkel cells (Extended Data Table 2)[17,18]. Notably, the characteristic dynamic response of SAM I fibres recorded from *Piezo2*^{CKO} mice was almost absent compared to controls with all velocity ramps tested (Fig. 3b–d); in addition, these fibres displayed markedly reduced static responses. The prominent deficit in slowly adapting Aβ fibres described here is consistent with the hypothesis that Piezo2 in both Merkel cells and sensory afferents contributes to SAM I firing activity[4,5]. Rapidly adapting mechanoreceptors that innervate hair follicles also increase their firing rates with increasing stimulus speed[19]. This velocity sensitivity was almost absent in the remaining rapidly adapting mechanoreceptors encountered in *Piezo2*^{CKO} mutant mice (Fig. 3e).

Examination of the mechanical thresholds and stimulus response functions of Aδ and C fibres revealed that Aδ mechanonociceptors exhibited elevated thresholds (Fig. 3f and Extended Data Fig. 5b), but the mechanosensitivity of C-fibre nociceptors were unaffected in *Piezo2*^{CKO} mutant mice (Fig. 3f and Extended Data Fig. 5c). Mechanoreceptors called D-hairs with Aδ-fibre axons were encountered less frequently in *Piezo2*^{CKO} mutant mice compared to controls but this did not reach statistical significance (Fisher's exact test, $P > 0.1$) (Extended Data Table 2), but the four fibres encountered showed stimulus response properties indistinguishable from those in controls (Extended Data Fig. 5d). Most C fibres are polymodal and respond to chemical and thermal stimuli in addition to mechanical pressure. Using a Peltier device, the thermal sensitivity of C fibres was tested, and both heat threshold for the first spike and the mean firing rates to the standard heat stimulus (ramp 1 °C per s, 32–48 °C) were unchanged in *Piezo2*^{CKO} mutant mice compared to controls (Fig. 3g and Extended Data Fig. 5e). Noxious cold sensitivity of *Piezo2*^{CKO} mutant C fibres was also unaffected (data not shown). We and others have recorded C fibres with very low mechanical thresholds in hairy skin, but their rarity precluded a detailed analysis as we did not encounter any in our control sample (Extended Data Table 2).

Our electrophysiological findings from hairy skin demonstrate that mechanosensitivity of DRG neurons to low threshold forces is predominately mediated by Piezo2; however, the mechanosensitivity of most nociceptors is largely unaffected in *Piezo2*^{CKO} mice. Any remaining mechanosensitivity in *Piezo2*^{CKO} Aβ fibres could be due to incomplete Piezo2 ablation in *Piezo2*^{CKO} mice or the presence of as-yet-unidentified mechanically activated ion channels. Our finding of an elevation in the mean mechanical threshold for activation of Aδ mechanonociceptors suggests that Piezo2 may contribute partly to mechanosensitivity of these neurons, a finding consistent with recent data indicating that single sensory neurons often possess multiple mechanosensitive currents[20].

We next performed a battery of behavioural assays to test innocuous and noxious mechanical and thermal sensitivities of *Piezo2*^{CKO} mice. We tested for the ability of *Piezo2*^{CKO} mice to detect von Frey filaments of varying forces applied to their hind paws[21]. Whereas *Piezo2*^{WT} mice showed a linear increase in detection of von Frey filaments from 1.0 g to 5.5 g, *Piezo2*^{CKO} mice were severely impaired in their ability to respond to forces below 4.0 g (Fig. 4a, see Methods for an explanation of the units used). Notably, *Piezo2*^{CKO} mice showed no differences in sensing the higher forces, highlighting the role of Piezo2 in a specific range of mechanical stimuli and indicating that *Piezo2*^{CKO} mice were able to perform motor functions. We then used the cotton swab assay where a sweeping motion of cotton underneath the mouse paw led to consistent withdrawal responses in *Piezo2*^{WT} mice, whereas *Piezo2*^{CKO} mice showed markedly reduced responses to the cotton swab stimulus (Fig. 4b)[22]. We also built a novel two-choice preference assay to evaluate innocuous mechanosensation (Extended Data Fig. 6a, b) and found that C57BL/6J mice consistently avoided the mechanically active side and spent time on the inactive side (Extended Data Fig. 6c)[23]. *Piezo2*^{WT} mice behaved similarly to C57BL/6J mice and showed robust avoidance behaviour to this stimulus, whereas the *Piezo2*^{CKO} mice showed no preference and spent equal time in the mechanically active and inactive sides (Fig. 4c).

In the assays described above, the paws of the mice receive the majority of the mechanical stimulation. We therefore tested the response of *Piezo2*^{CKO} mice to a mechanical stimulus given to hairy skin. We used a modified version of the tape response assay to monitor the response of mice to adhesive tape attached to their back[24]. *Piezo2*^{WT} mice showed

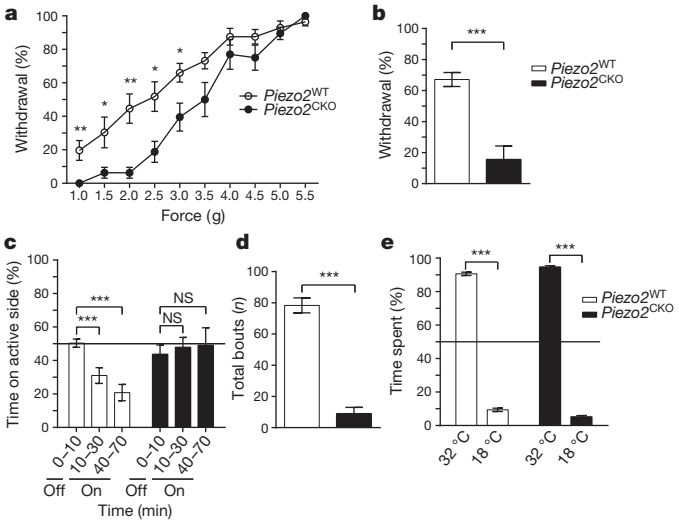

Figure 4 | *Piezo2*^{CKO} mice show profound and specific defects in innocuous touch sensation in multiple behavioural assays. **a**, Per cent response to varying forces (see Methods for an explanation of the units) of von Frey filaments in *Piezo2*^{WT} ($n = 14$) and *Piezo2*^{CKO} mice ($n = 12$). **b**, Per cent response to a sweep of a cotton swab on the hind paw in *Piezo2*^{WT} ($n = 14$) and *Piezo2*^{CKO} mice ($n = 9$). Of note, 6 out of 9 *Piezo2*^{CKO} mice showed zero responses to the cotton stimulus. **c**, Measurement of time spent in a behavioural assay where mice are placed in an apparatus consisting of two platforms, with one side mechanically active and the other side kept still. For the first 10 min, no stimulation is given to either side ('off') to allow for acclimation. Mechanical stimulation is then provided to one side for 1 hour and per cent time spent on the two sides is plotted, *Piezo2*^{WT} ($n = 15$) and *Piezo2*^{CKO} mice ($n = 11$). **d**, Number of bouts in response to a 3 cm piece of adhesive tape affixed to the back of a mouse over a 5 min period in *Piezo2*^{WT} ($n = 14$) and *Piezo2*^{CKO} mice ($n = 10$). **e**, Percentage of time spent on either side of a two-choice assay with one zone set at 18 °C and one zone set at 32 °C in *Piezo2*^{WT} ($n = 13$) and *Piezo2*^{CKO} mice ($n = 10$). Error bars represent s.e.m., all experiments performed with at least four separate cohorts of both male and female littermate control mice, $*P < 0.05$, $**P < 0.005$, $***P < 0.0005$, Mann–Whitney non-parametric analysis.

clear responses to the tape and made ~80 attempts to remove the tape over the course of 5 min. *Piezo2*^{CKO} mice barely responded to this stimulus (Fig. 4d). These data demonstrate that *Piezo2*^{CKO} mice have a dramatic inability to sense innocuous touch. Notably, when Piezo2 is deleted in epidermal Merkel cells but not in DRG neurons using the *K14-cre* line, these mice had a slight defect in response to von Frey filaments, but no defects in the other three innocuous touch behavioural assays described here (data not shown)[4]. Importantly, to confirm that this behaviour is not due to Piezo2 deletion in non-sensory tissues, we performed immunostaining using the *Piezo2-GFP* reporter mouse line and were unable to detect Piezo2 expression in motor neurons, cerebellum or skeletal muscle (data not shown). Therefore, the considerably more pronounced behavioural deficits resulting from Piezo2 deletion in *Advil-creERT2* mice emphasize the primary role of sensory neurons in touch sensation.

We then investigated whether *Piezo2*^{CKO} mice are able to respond to thermal stimuli and noxious mechanical forces. *Piezo2*^{CKO} mice showed no differences compared to littermate controls in innocuous temperature sensation, demonstrating that the deficits in mechanical insensitivity are not due to general health issues (Fig. 4e)[23]. To determine whether *Piezo2*^{CKO} mice could respond to noxious mechanical stimuli, we first used a ramping von Frey protocol and found that *Piezo2*^{CKO} mice showed no differences in response threshold compared to *Piezo2*^{WT} mice (Extended Data Fig. 7a). These results are in line with the static force von Frey assay where the major deficit was observed only for low-threshold stimuli. *Piezo2*^{CKO} mice also showed similar responses to *Piezo2*^{WT} mice in noxious force sensing assays such as tail clip and the Randall–Selitto test (Extended Data Fig. 7b, c). Furthermore, we observed no differences to noxious temperature sensitivity between control and *Piezo2*^{CKO} mice (Extended Data Fig. 7d). Recent reports have suggested a role for Piezo2 in mechanical allodynia[12,25]. Although Piezo2 activity is sensitized in response to inflammatory signals *in vitro*, we did not observe any behavioural deficits in mechanical nociception or mechanical allodynia in response to inflammatory mediators in *Piezo2*^{CKO} mice (Extended Data Fig. 7e, f)[10]. Future studies are needed to explore Piezo2 mechanical sensitivity in response to nerve injury.

Ion channels responsible for detecting mechanical stimuli relevant for somatosensation have long been sought, and our results demonstrate that Piezo2 is the major mechanotransducer required for touch sensation in mammals. The loss of the MEC-2-related protein STOML3 also leads to loss of mechanoreceptor sensitivity[15,20] and recent data show that this protein is a powerful positive modulator of Piezo channel mechanosensitivity. We show that Piezo2-dependent rapidly adapting, mechanically activating currents *in vitro* account for the mechanosensitivity of the majority of LTMRs without affecting the function of nociceptors. It is interesting that a Piezo2-mediated rapidly adapting current *in vitro* can account for both rapidly and slowly adapting fibre responses *in vivo*. At least in Merkel cells, the small remaining Piezo2-mediated current during long-lasting stimulations is sufficient to produce large sustained depolarization, probably due to the high membrane resistance of these cells, which leads to slowly adapting responses in sensory afferents[4,5]. Our electrophysiological results are unambiguously supported by behavioural studies that show an almost complete deficit in touch sensation without affecting pain sensation in Piezo2-deficient mice, and predict the existence of other mechanotransducers relevant for pain sensation. Piezo1, a related mechanosensitive ion channel required for vascular development, is not expressed at significantly high levels in sensory neurons to be a likely candidate (Extended Data Fig. 8a, b)[26]. Ion channels that sense cell volume, such as the recently identified SWELL1, might also play a role in nociception[27,28]. Furthermore, the as-yet-unknown cationic channels that account for the intermediately and slowly adapting, mechanically activated currents in cultured DRGs (Fig. 2d) are likely to be involved in nociception. Different mechanotransducers also account for innocuous and noxious mechanosensation in *Drosophila*[2]. Notably, *Drosophila* Piezo is required for mechanical nociception, and not for gentle touch sensation[29]. Regardless, our findings highlight the role of Piezo proteins as evolutionarily conserved mechanically activated ion channels involved in somatosensory mechanotransduction from flies to mammals[29,30].

Online Content Methods, along with any additional Extended Data display items and Source Data, are available in the online version of the paper; references unique to these sections appear only in the online paper.

Received 2 July; accepted 17 October 2014.

1. Abraira, V. E. & Ginty, D. D. The sensory neurons of touch. *Neuron* **79,** 618–639 (2013).
2. Árnadóttir, J. & Chalfie, M. Eukaryotic mechanosensitive channels. *Annu. Rev. Biophys.* **39,** 111–137 (2010).
3. Coste, B. *et al.* Piezo1 and Piezo2 are essential components of distinct mechanically activated cation channels. *Science* **330,** 55–60 (2010).
4. Woo, S.-H. *et al.* Piezo2 is required for Merkel-cell mechanotransduction. *Nature* **509,** 622–626 (2014).
5. Maksimovic, S. *et al.* Epidermal Merkel cells are mechanosensory cells that tune mammalian touch receptors. *Nature* **509,** 617–621 (2014).
6. Ikeda, R. *et al.* Merkel cells transduce and encode tactile stimuli to drive Aβ-afferent impulses. *Cell* **157,** 664–675 (2014).
7. Maricich, S. M., Morrison, K. M., Mathes, E. L. & Brewer, B. M. Rodents rely on Merkel cells for texture discrimination tasks. *J. Neurosci.* **32,** 3296–3300 (2012).
8. Lechner, S. G. & Lewin, G. R. Hairy sensation. *Physiology (Bethesda)* **28,** 142–150 (2013).
9. Maksimovic, S., Baba, Y. & Lumpkin, E. A. Neurotransmitters and synaptic components in the Merkel cell-neurite complex, a gentle-touch receptor. *Ann. NY Acad. Sci.* **1279,** 13–21 (2013).
10. Dubin, A. E. *et al.* Inflammatory signals enhance piezo2-mediated mechanosensitive currents. *Cell Rep.* **2,** 511–517 (2012).
11. Haeberle, H. *et al.* Molecular profiling reveals synaptic release machinery in Merkel cells. *Proc. Natl Acad. Sci. USA* **101,** 14503–14508 (2004).

12. Lou, S., Duan, B., Vong, L., Lowell, B. B. & Ma, Q. Runx1 controls terminal morphology and mechanosensitivity of VGLUT3-expressing C-mechanoreceptors. *J. Neurosci.* **33,** 870–882 (2013).
13. McCarter, G. C., Reichling, D. B. & Levine, J. D. Mechanical transduction by rat dorsal root ganglion neurons *in vitro*. *Neurosci. Lett.* **273,** 179–182 (1999).
14. Hu, J. & Lewin, G. R. Mechanosensitive currents in the neurites of cultured mouse sensory neurones. *J. Physiol.* **577,** 815–828 (2006).
15. Wetzel, C. *et al.* A stomatin-domain protein essential for touch sensation in the mouse. *Nature* **445,** 206–209 (2007).
16. Moshourab, R. A., Wetzel, C., Martinez-Salgado, C. & Lewin, G. R. Stomatin-domain protein interactions with acid-sensing ion channels modulate nociceptor mechanosensitivity. *J. Physiol.* **591,** 5555–5574 (2013).
17. Maricich, S. M. *et al.* Merkel cells are essential for light-touch responses. *Science* **324,** 1580–1582 (2009).
18. Wellnitz, S. A., Lesniak, D. R., Gerling, G. J. & Lumpkin, E. A. The regularity of sustained firing reveals two populations of slowly adapting touch receptors in mouse hairy skin. *J. Neurophysiol.* **103,** 3378–3388 (2010).
19. Rugiero, F., Drew, L. J. & Wood, J. N. Kinetic properties of mechanically activated currents in spinal sensory neurons. *J. Physiol. (Lond.)* **588,** 301–314 (2010).
20. Poole, K., Herget, R., Lapatsina, L., Ngo, H. D. & Lewin, G. R. Tuning Piezo ion channels to detect molecular-scale movements relevant for fine touch. *Nature Commun.* **5,** 3520 (2014).
21. Petrus, M. *et al.* A role of TRPA1 in mechanical hyperalgesia is revealed by pharmacological inhibition. *Mol. Pain* **3,** 40 (2007).
22. Garrison, S. R., Dietrich, A. & Stucky, C. L. TRPC1 contributes to light-touch sensation and mechanical responses in low-threshold cutaneous sensory neurons. *J. Neurophysiol.* **107,** 913–922 (2012).
23. Dhaka, A. *et al.* TRPM8 is required for cold sensation in mice. *Neuron* **54,** 371–378 (2007).
24. Bradbury, E. J. *et al.* Chondroitinase ABC promotes functional recovery after spinal cord injury. *Nature* **416,** 636–640 (2002).
25. Eijkelkamp, N. *et al.* A role for Piezo2 in EPAC1-dependent mechanical allodynia. *Nature Commun.* **4,** 1682 (2013).
26. Ranade, S. S. *et al.* Piezo1, a mechanically activated ion channel, is required for vascular development in mice. *Proc. Natl Acad. Sci. USA* **111,** 10347–10352 (2014).
27. Voss, F. K. *et al.* Identification of LRRC8 heteromers as an essential component of the volume-regulated anion channel VRAC. *Science* **344,** 634–638 (2014).
28. Qiu, Z. *et al.* SWELL1, a plasma membrane protein, is an essential component of volume-regulated anion channel. *Cell* **157,** 447–458 (2014).
29. Kim, S. E., Coste, B., Chadha, A., Cook, B. & Patapoutian, A. The role of *Drosophila* Piezo in mechanical nociception. *Nature* **483,** 209–212 (2012).
30. Faucherre, A., Nargeot, J., Mangoni, M. E. & Jopling, C. *piezo2b* regulates vertebrate light touch response. *J. Neurosci.* **33,** 17089–17094 (2013).

Acknowledgements We acknowledge T. Goode for help in behavioural analysis. We also thank R. Moran and T. Johnson for assistance with histology, K. Spencer for imaging analysis and M. Braunschweig for technical assistance. S.S.R. was funded by a pre-doctoral fellowship from the California Institute of Regenerative Medicine. R.A.M. was supported by Clinical Research Fellowship from the Max Delbrück Center (MDC). G.R.L.'s laboratory was supported by senior European Research Council grant (project 294678) and a grant from the Deutsche Forschungsgemeinshaft (SFB958 project A9). A.P. is a Howard Hughes Medical Institute Investigator. This study was partly funded by NIH grant R01 DE022358 to A.P.

Author Contributions S.S.R. and A.P. designed experiments and wrote the manuscript along with G.R.L. S.S.R., J.N.W. and Z.Q. generated transgenic lines used in this study. S.-H.W. performed all immunostaining experiments. A.E.D. conducted electrophysiology on cultured DRG neurons and J.M. isolated and cultured cells. R.A.M., C.W., V.B. and G.R.L. performed skin nerve electrophysiology and analysed the data. S.S.R., M.P., A.G.F. and K.R. performed behavioural assays on mice. B.C., J.M. and A.J.W. developed the novel two-choice mechanosensory instrument.

Author Information Reprints and permissions information is available at www.nature.com/reprints. The authors declare no competing financial interests. Readers are welcome to comment on the online version of the paper. Correspondence and requests for materials should be addressed to A.P. (ardem@scripps.edu).

METHODS

All animal procedures were approved by TSRI Institutional Animal Care and Use Committees or were approved by the animal welfare office of federal state of Berlin.

Immunofluorescence. Dorsal root ganglia neurons (DRG), dorsal skin and footpads were collected from 7-week-old mice. Tissues were briefly fixed in 4% PFA and were processed as previously described[4]. Fluorescent images were captured using a Nikon confocal microscope C2. Antibodies used for immunofluorescence staining were previously reported with the addition of thymidine hydroxylase (Millipore) and CGRP (Abcam)[4]. Immunostaining images from Ai9 reporter mice crossed with the *Advil-creERT2* line were visualized by tdTomato epifluorescence[31,32].

Cell culture and small interfering RNA of DRG neurons. DRG cultures and transfection of short interfering RNA (siRNA) (for Piezo1 experiments) were performed exactly as previously described[3]. Reagents: mouse Piezo1 siRNA smart pool Dharmacon (ON-TARGETplus mouse Piezo1 (234839) siRNA SMARTpool; catalog no. L-061455-00-0005); scramble siRNA controls, Qiagen Allstars Negative Control (SI03650318).

***In situ* hybridization.** DRG neurons from C57BL/6J mice were harvested from all levels and fixed in 10% formalin overnight. The DRG neurons were then dehydrated through an ethanol series/xylene and embedded in paraffin. Ten-micrometre sections were cut and *in situ* hybridization was carried out using the RNAscope assay (Advanced Cell Diagnostics; Hayward, CA) according to the manufacturer's instructions. Development of signal was performed using the RNAscope 2.0 HD brown detection kit. Probes for mPiezo1 (cat. number: 400181) and mPiezo2 (cat. number: 400191) were purchased from Advanced Cell Diagnostics (Hayward, CA). Slides were mounted with Cytoseal and imaged under a bright field microscope. Slides were scanned and images captured using the Nanozoomer 2.0 HT (Hamamatsu).

Electrophysiology. Whole-cell patch clamp recordings were performed as described using standard methods to achieve low access resistance[4,10]. Cells were maintained at 22–24 °C in: 127 mM NaCl, 3 mM KCl, 1 mM $MgCl_2$, 2.5 mM $CaCl_2$, 10 mM dextrose, 10 mM HEPES (pH 7.3). Electrodes had resistances of 4.6 ± 0.7 MΩ (n = 117) when filled with gluconate-based low chloride intracellular solution: 125 mM K-gluconate, 7 mM KCl, 1 mM $CaCl_2$, 1 mM $MgCl_2$, 10 mM HEPES, 1 mM tetraK-BAPTA, 4 mM Mg-ATP, 0.5 mM Na-GTP (pH 7.3 with KOH). Neurons with diameters of 14 to 41 μm were tested for mechanosensitivity using a fire-polished glass probe; the average cell diameter was similar among genotypes (23.1 ± 0.8 μm (n = 57) and 22.7 ± 0.7 μm (n = 62), respectively). The probe displacement was advanced in increments of 0.5 or 1 μm. All data were analysed as previously described[3,10].

***Ex vivo* skin nerve preparation.** The skin nerve preparation was used essentially as previously described to record from single primary afferents[16]. Mice were euthanized by CO_2 inhalation for 2–4 min followed by cervical dislocation. The saphenous nerve and the shaved skin of the hind limb were dissected free and placed in an organ bath at 32 °C. The chamber was perfused with a synthetic interstitial fluid (SIF buffer): 123 mM NaCl, 3.5 mM KCl, 0.7 mM $MgSO_4$, 1.7 mM NaH_2PO_4, 2.0 mM $CaCl_2$, 9.5 mM sodium gluconate, 5.5 mM glucose, 7.5 mM sucrose, and 10 mM HEPES (pH 7.4). The skin was placed with the corium side up in the organ bath. The saphenous nerve was placed in an adjacent chamber on a mirror to aid and under microscopy fine filaments were teased from the nerve and placed on the recording electrode. Electrical isolation was achieved with mineral oil.

For the electrical search protocol a microelectrode (0.5–1 MΩ) was manoeuvred gently to contact the epineurium of saphenous nerve and deliver electrical stimulations at 1 s intervals with square pulses of 50–500 ms duration. In most filaments 5–7 single units were encountered. The electrical nerve stimulation was done at up to 3 sites (corresponding to major branching points of the saphenous nerve) to trace electrically identified units to their receptive fields. Mechanical sensitivity of single units was tested by mechanical stimulation of their receptive field with a glass rod; units not responding to mechanical probing were designated as mechano-insensitive. Based on the conduction velocity, these units were categorized as mechanically insensitive Aβ, Aδ and C fibres.

Mechanically sensitive units were characterized by conduction velocity (calculated by dividing conduction distance over electrical latency for the spike) and stimulus response function was obtained by a standardized mechanical stimulation protocol. The stimulating probe, equipped with a force transducer (Kleindiek, Reutlingen, Germany), was placed onto a spot within the receptive field where the most reliable responses could be obtained. The probe was a stainless steel metal rod and the diameter of the flat circular contact area was 0.8 mm. Two mechanical stimulation protocols were employed. The first stimulation protocol was applied to SAM, RAM and D-hair receptors. A piezo actuator (Physik Instrumente) was used to deliver five ramp and hold stimuli (90 μm displacement, 2 s hold-phase and 30 s interstimulation interval) with increasing ramp velocities (0.075, 0.15, 0.45, 1.5 and 15 mm s^{-1}). The second stimulation protocol was applied to Aδ mechanonociceptors and C fibres and consisted of an ascending series (6 ramp and hold stimuli) of 10 s displacement stimuli (32–1,024 μm) at 30-s intervals, sent as a pre-programmed series of commands to a computer-controlled nanomotor (Kleindiek, Reutlingen, Germany). Mechanical thresholds for nociceptors were measured by reading off the force (obtained from the attached force transducer) at which the first spike was obtained. The signal driving the movement of the linear motor and raw electrophysiological data were collected with a Powerlab 4.0 system (ADInstruments) and spikes were discriminated off-line with the spike histogram extension of the software. Data were obtained from between 6 and 20 skin nerve preparations per genotype.

Tamoxifen injections. Fifteen milligrams of tamoxifen (Sigma) was dissolved into 1 ml of 100% corn oil and made fresh daily before use. *Piezo2*^{WT} and *Piezo2*^{CKO} mice both received tamoxifen injections (intraperitoneal) at 150 mg kg^{-1} for 5 consecutive days. Due to variability in tamoxifen injections and the observation of incomplete deletion in *Piezo2*$^{fl/fl}$ mice, *Piezo2*$^{fl/-}$ mice, containing one floxed allele and one null allele, were used for analysis. *Piezo2*^{CKO} refers to mice that received tamoxifen injections. Each mouse was weighed before injection to normalize for differences in body weight. Somatosensory behavioural assays were performed on mice between 7 and 21 days after tamoxifen injections, and all mice that were tested for mechanical sensitivity were also tested for thermal sensitivity to control for any issues of general health. Before tamoxifen injections, *Piezo2*^{CKO} mice were healthy and viable with no differences compared to *Piezo2*^{WT} littermate controls in various somatosensory assays (data not shown). However, tamoxifen injections led to a visible difference in behaviour of *Piezo2*^{CKO} but not *Piezo2*^{WT} mice that started ~7 days after the last injection. *Piezo2*^{CKO} mice walked with an irregular gait, sometimes dragged their hind legs, and were occasionally uncoordinated when attempting to stand on their hind legs.

Quantitative real-time PCR analysis. qPCR analysis was performed by first isolating total RNA using TRIzol/chloroform and isopropanol precipitation from freshly isolated DRG neurons (Life Technologies). Generation of complementary DNA was achieved by reverse transcription using the QuantiTect Reverse Transcript kit (Qiagen). For qPCR, FastStart Universal probe master mix (Rox) from Roche Diagnostics was used. The reaction was run in the Eco Real-Time PCR instrument (Illumina) using 0.5 μl of the cDNA in a 10 μl reaction according to the manufacturer's instructions. Real-time Taqman qPCR assays were purchased from Integrated DNA Technologies with a FAM reporter dye and a non-fluorescent quencher: mouse *Piezo2* (Mm.PT.56a.32860700, Fam38b), and an internally designed mouse *Gapdh* assay (forward primer: GCACCACCAACTGCTTAG; reverse primer: GGATG CAGGGATGATGTTC; and probe: CAGAAGACTGTGGATGGCCCCTC).

Calibrations and normalizations were done using the $2^{-\Delta\Delta C_T}$ method, where $\Delta\Delta C_T = ((C_T \text{ (target gene)} - C_T \text{ (reference gene)}) - (C_T \text{ (calibrator)} - C_T \text{ (reference gene)})$. *Gapdh* was used as the reference gene for all qPCR experiments[33].

Static force von Frey. Responses to application of a von Frey filament was performed as previously described[21,34]. Mice are acclimated in an elevated platform for 1 h, in a similar manner to that described for the cotton swab assay. A Dynamic Plantar Aesthesiometer is used to apply varying forces of a 0.5 mm von Frey filament (Ugo Basile product ID 37450). A single force is applied for one second to the hind paw and a yes/no withdrawal response is scored. Forces on the instrument are measured with units 'g' and represent grams-force, according to manufacturer's description (Ugo Basile). The initial force applied is 5.5 g and is lowered incrementally by 0.5 g, and testing ends after reaching 1.0 g. The fraction of the number of responses out of four applications per force is measured. Data are plotted as percentage of withdrawal at each force for control and test mice.

Two-choice mechanosensory assay. The novel two-choice mechanosensory assay instrument consists of two lightweight, stiff, composite platforms which are separately activated by a pair of tactile transducers (Clark Instruments). The platforms are mounted to a frame via low rate coil springs. The springs act to mechanically isolate the platforms from each other and the frame. A thin sheet of silicone rubber is fastened to the tops of the platforms and the frame. This provides a continuous surface that covers the gaps between the frame and platforms. Dividers are placed on top of the frame to create lanes. A clear plastic cover sits on all lanes to prevent mice from climbing out of the lane. Tactile transducers housed underneath the platforms are connected to a two-channel amplifier which is fed the appropriate sine wave signals via a Labview-controlled signal generator.

For behavioural analysis, individual mice were placed in one of six lanes, with a maximum of six mice tested at the same time. We optimized the output of the stimulator using multiple protocols and found that C57BL/6J mice consistently avoided the active side when using a protocol of 150 Hz (sine wave), at a peak-to-peak displacement of 33.1 μm and a pulsing stimulus of 3 s on and 2 s off. Interestingly, mice showed decreased avoidance of the active side when the vibration stimulus was kept constant. A side at random was turned off and the other side was turned on to a pulsing stimulus. The acceleration and frequency produced were monitored using a custom-designed program (Dual Channel v.7) to ensure only one side was active. Mice were allowed to walk freely between two zones for 10 min with no stimulus and were assayed for 1 h with the pulsing protocol. EthoVision tracking system (Noldus Information Technology) was used to monitor the movement of the mice in a dark

room illuminated with infrared light. Data are plotted as the percentage of the time spent on the active zone.

Cotton swab assay. A method to assess light-touch-evoked paw withdrawal was used as described previously[22]. Mice were placed in an elevated acclimation chamber separated by plexiglass dividers. The floor consists of mesh-like grids that are accessible from below due to small gaps of ~5 × 5 mm (Ugo Basile product ID 37450-277). Mice are allowed to acclimate for 1 h before testing. A cotton swab from a Q-tip is manually pulled so that it is 'puffed out' to ~3× the original size. A sweeping motion, rather than an upward motion, is used underneath the mouse paw and mice are assayed for a paw withdrawal response. Five sweeps are performed with at least 10 s between each sweep. The number of withdrawals out of five trials are counted and recorded as a percentage for each mouse.

Tape response assay. A modified version of the tape on paw assay was performed[24]. Mice are allowed to acclimate in a circular plexiglass container for 5 min. A 3 cm piece of common laboratory tape was then applied gently to the back of the mouse such that it sticks to the mouse. Mice are then observed for 5 min and the total number of responses to the tape are counted. A response is scored when the mouse stops moving and bites or scratches the piece of tape or shows a visible 'wet dog shake' motion in an attempt to remove the foreign object on its back.

Ramping von Frey. Measurement of a response to a von Frey filament was performed as previously described[21]. Mice are acclimated and tested using the same Dynamic Plantar Aesthesiometer as described for static force von Frey (Ugo Basile). Instead of a static force application as described above, a ramping protocol is used that increases in force gradually from 0–50 g over the course of 20 s. The von Frey filament is applied until the mouse withdraws its hind paw. Each mouse receives four applications of the von Frey filament and the average force (threshold for withdrawal) is plotted for each mouse.

Hargreaves assay. A paw withdrawal response to infrared light is performed as previously described[21]. Mice are allowed to acclimate on a plexiglass container with a clear flat bottom for at least 60 min. The infrared light heat source is set to an intensity of 20, according to manufacturer's protocols (Ugo Basile product ID 37370). The heat source is placed under the platform where mice are acclimated and the light is applied to the hind paw. The time to paw withdrawal is measured and repeated three times for each mouse with a cutoff of 20 s. The average time to withdrawal (latency) is plotted for each mouse.

Randall–Selitto assay. Response to a noxious level of pinching force on the paw of a mouse was performed as previously described[34]. Mice are placed into a small sling that allows the mice to be restrained and the paws to be accessible (IITC Life Sciences). A pinching force is applied to the hind paw using a Randall–Selitto device (IITC Life Sciences). Three separate pinches are applied where the force increases until reaching a 300 *g* cutoff. A response is scored by any visible flinch or audible vocalization. Data are plotted as the average of three responses (threshold) calculated for each mouse.

Tail clip assay. An assay to determine the time for response to an alligator clip placed on the tail of a mouse was slightly modified from ref. 35. An alligator clip commonly used for electrical wires was purchased from The Home Depot. The clips were altered by filing down the sharp teeth and then covered with a rubber casing to reduce the potential for tissue damage. We calibrated the strength of the force exerted by the clips to be 500 g. The clips were marked at the centre to ensure placement of the clip was similar for all mice tested. The clips are placed near the base of the mouse tail and then the mice are placed on a table inside a plexiglass container. A response was scored when the mice showed awareness of the clip by biting, vocalization, grasping of tail or a jumping response. Data are plotted as the time to respond (latency) for each mouse.

Complete Freund's adjuvant with von Frey. A standard assay for inflammation due to complete Fruends adjuvant (CFA) injection in the hindpaw was performed as previous described[21]. Mice were subjected to ramping von Frey (detailed above) before injection of CFA. After baseline analysis, mice were injected in the hind paw with 10 µl of CFA (Sigma). Mice were then rehoused in their home cages and tested by ramping von Frey the following day, 24 h post injection.

Bradykinin with von Frey. Inflammation response to bradykinin injection was performed as previously described[21]. Animals were acclimated and tested by ramping von Frey (detailed above). After baseline analysis was performed, mice were injected with 20 µl of bradykinin (10 nM). Mice were then placed back in the acclimation chambers and tested by ramping von Frey at 5, 10 and 15 min post injection.

Two temperature choice assay. A preference assay between 32 °C and 18 °C was performed as previously described[23]. Mice were placed on a platform where plexiglass dividers separated the entire platform into six lanes. The platform was divided into two zones such that one side was heated to 32 °C and the other side was cooled to 18 °C. One mouse was placed in each lane and allowed to walk freely between the two zones for 1 h. An automated tracking device (Noldus Ethovision software) monitored the movement of the mice in a dark room illuminated with infrared light. Data are plotted as the percentage of time spent on the 32 °C zone versus the 18 °C zone.

Statistics. All data analysed by statistical analyses are detailed in the figure legends. Data from electrophysiological analysis and qPCR of isolated DRG experiments were analysed by Student's *t*-test as previously described[3]. Electrophysiological skin nerve data were analysed using Fischer's exact test, Fig. 3a; Mann–Whitney test, Fig. 3f, g, h; and repeated measures ANOVA, Fig. 3d, e. For all behavioural experiments, the Mann–Whitney non-parametric statistical test was used.

Sample size choice. The specific number of independent experiments or animal numbers used for all experiments is outlined in the corresponding figure legends. For electrophysiology and qPCR of DRG experiments, data were analysed from $n = 3$ independent experiments. For skin nerve preparations data was obtained from between 6 and 20 skin nerve preparations per genotype. All behavioural data represent results from 2–4 independent rounds of testing with multiple mice of both genotypes per cohort. All mice tested in behavioural assays were littermate controls. Male and female mice were tested between the ages of 6–12 weeks. Animals were randomly chosen for experimental subjects and all experimental procedures were performed in a blinded manner. No statistical method was used to predetermine sample size.

31. Madisen, L. *et al.* A robust and high-throughput Cre reporting and characterization system for the whole mouse brain. *Nature Neurosci.* **13,** 133–140 (2010).
32. Lau, J. *et al.* Temporal control of gene deletion in sensory ganglia using a tamoxifen-inducible *Advillin-Cre-ERT2* recombinase mouse. *Mol. Pain* **7,** 100 (2011).
33. Livak, K. J. & Schmittgen, T. D. Analysis of relative gene expression data using real-time quantitative PCR and the $2^{-\Delta\Delta C_T}$ method. *Methods* **25,** 402–408 (2001).
34. Kwan, K. Y. *et al.* TRPA1 contributes to cold, mechanical, and chemical nociception but is not essential for hair-cell transduction. *Neuron* **50,** 277–289 (2006).
35. Lariviere, W. R. *et al.* Heritability of nociception. III. Genetic relationships among commonly used assays of nociception and hypersensitivity. *Pain* **97,** 75–86 (2002).

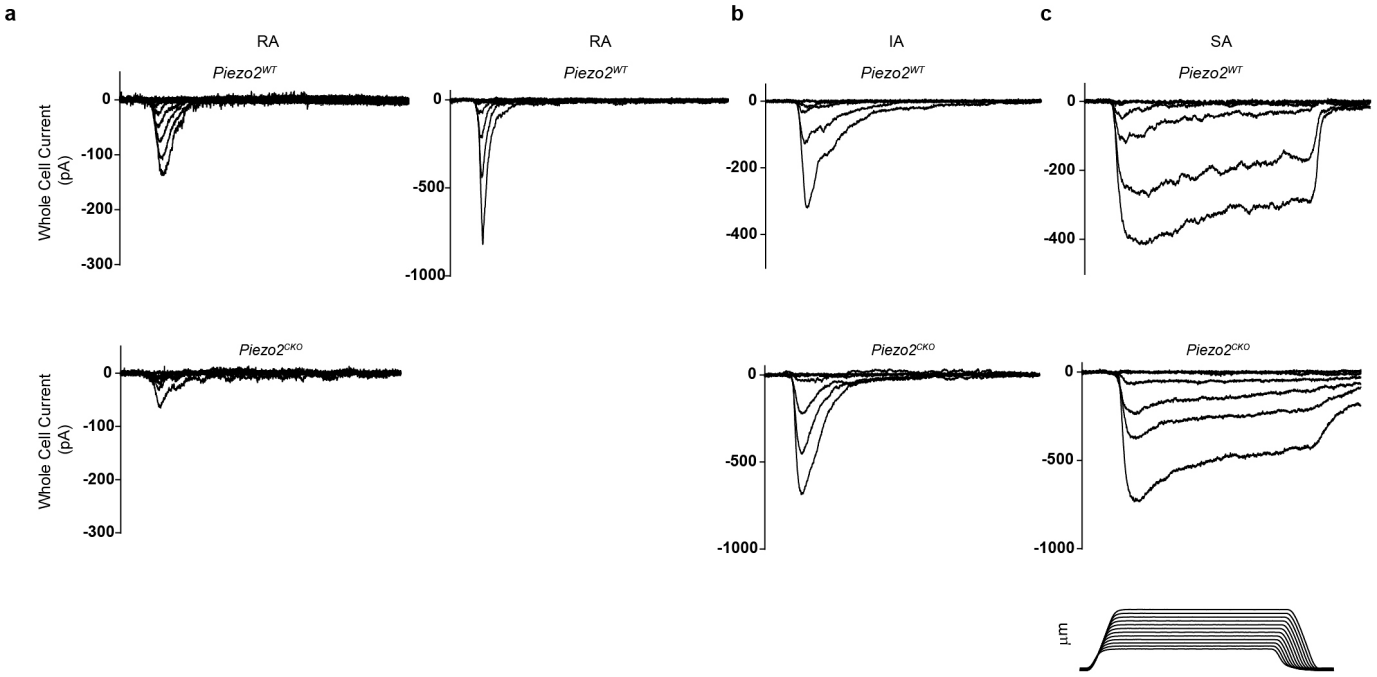

Extended Data Figure 1 | Mechanically activated currents elicited in cultured DRG neurons from *Piezo2*^{WT} and *Piezo2*^{CKO} mice by poking with a blunt probe. **a**, Representative traces of rapidly adapting (RA) currents in *Piezo2*^{WT} (top) and *Piezo2*^{CKO} (bottom). *Piezo2*^{WT} DRG neurons show characteristic rapidly adapting currents; a subpopulation can be active with apparent low thresholds (right). *Piezo2*^{CKO} mice contained a few rapidly adapting type cells but none appeared to be low-threshold mechanoreceptors. **b**, **c**, Representative traces of intermediately adapting (IA) and slowly adapting (SA) currents, respectively, with no observable differences between the two genotypes. All data were low-pass filtered off line at 4 kHz. Action potentials were elicited by current injection in all neurons. *Piezo2*^{WT}: RA, left: 20 µm diameter, 5 µm apparent threshold; RA, right: 28 µm diameter, 1 µm apparent threshold; IA: 23 µm diameter, 6 µm apparent threshold; SA: 20 µm diameter; 2 µm apparent threshold. *Piezo2*^{CKO}: RA, left: 23 µm diameter, 8 µm apparent threshold; RA, right: none found; IA: 20 µm diameter, 5.5 µm apparent threshold; SA: 30 µm diameter, 8 µm apparent threshold. Lower right shows an example of the probe displacement protocol (stimulus). Results from $n = 3$ independent experiments.

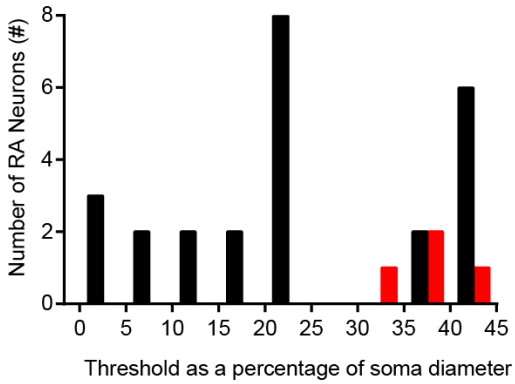

Extended Data Figure 2 | Apparent threshold analysis of *Piezo2*^{WT} and *Piezo2*^{CKO} DRG neurons. The smallest soma indentation eliciting a detectable mechanically activated response (apparent threshold) depends, in part, on the incremental distance applied (0.5 μm) and the proportional displacement in relation to the soma diameter. The apparent thresholds of all rapidly adapting responses normalized to soma diameter reveal a wide range of sensitivities of *Piezo2*^{WT} DRG neurons (black) and the high apparent threshold responses of the remaining rapidly adapting neurons in *Piezo2*^{CKO} DRG neurons (red). The lowest apparent thresholds are observed only in *Piezo2*^{WT}. Results from $n = 3$ independent experiments.

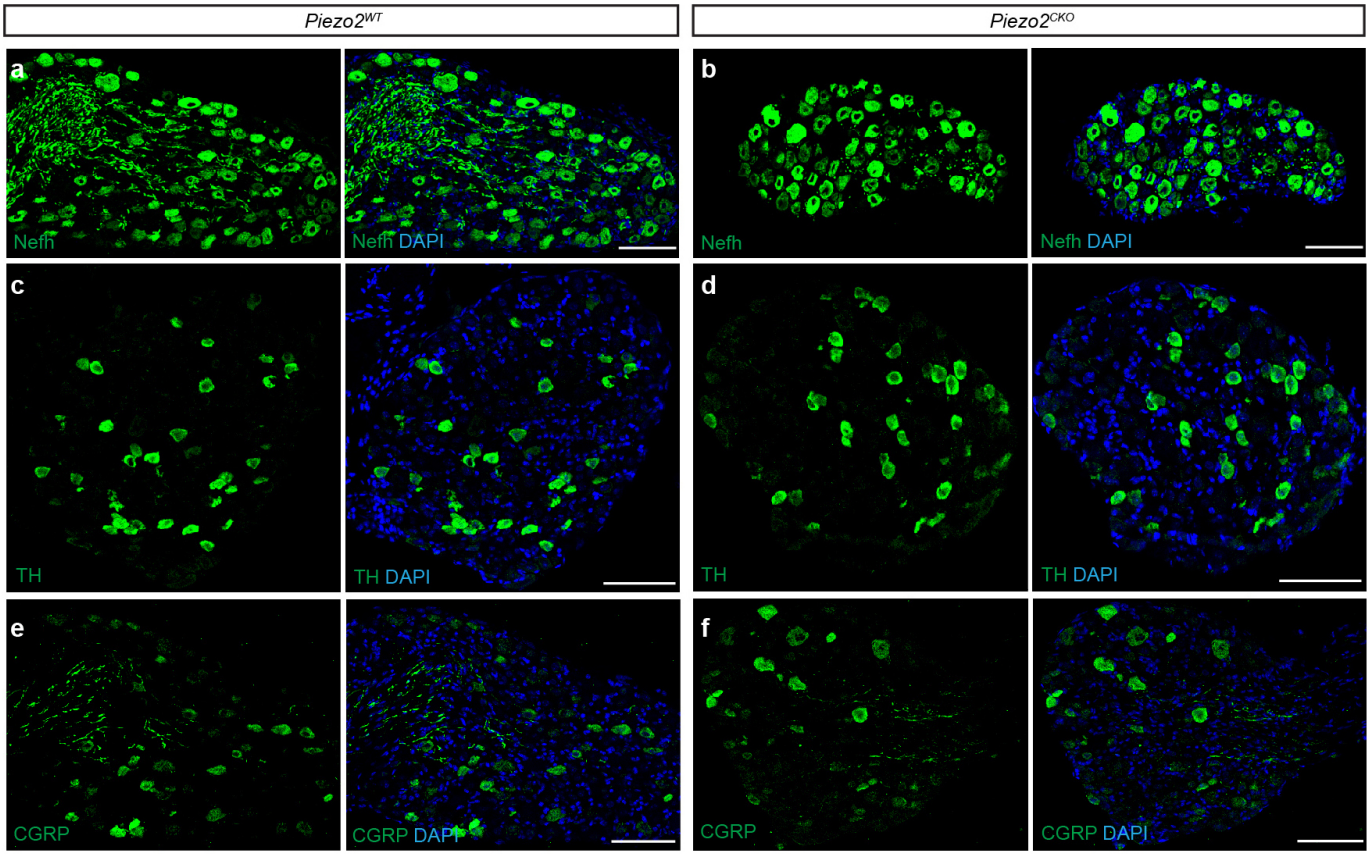

Extended Data Figure 3 | Expression of various markers of subpopulations of DRG neurons are similar in *Piezo2*^{WT} and *Piezo2*^{CKO} mice.
a, **b**, Representative images from immunofluorescence of Nefh in DRGs from *Piezo2*^{WT} (**a**) or *Piezo2*^{CKO} (**b**) mice. **c**, **d**, Representative image from immunofluorescence of thymidine hydroxylase (TH) in DRGs from *Piezo2*^{WT} (**c**) or *Piezo2*^{CKO} (**d**) mice. **e**, **f**, Representative image from immunofluorescence of CGRP in DRGs from *Piezo2*^{WT} (**e**) or *Piezo2*^{CKO} (**f**) mice. All markers stained in green. Scale bars, 100 μm.

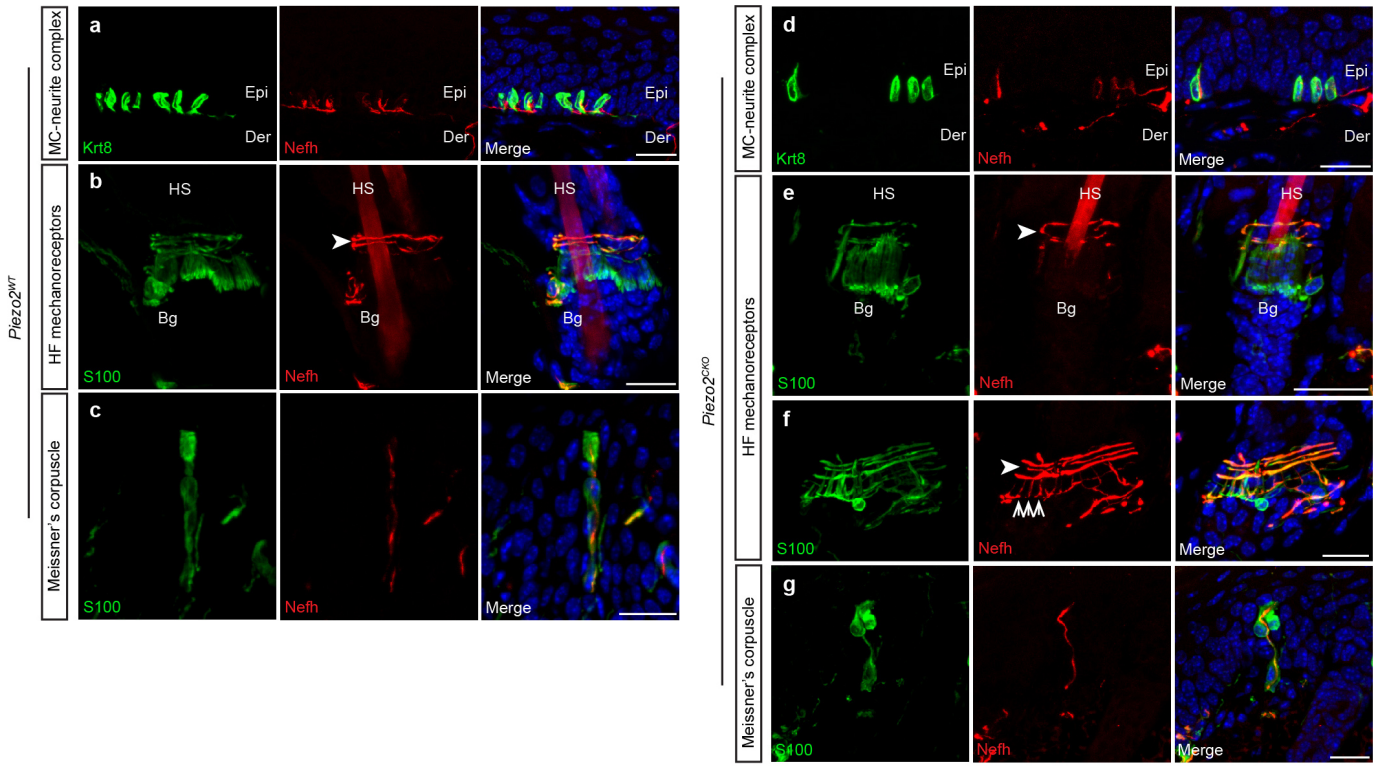

Extended Data Figure 4 | DRG innervation of skin is unaffected in *Piezo2*^{CKO} mice. **a**, **d**, Representative image of immunostaining of Krt8 (green) and Nefh (red) in Merkel-cell–neurite complexes in *Piezo2*^{WT} (**a**) and *Piezo2*^{CKO} (**d**) glabrous skin. **b**, **e**, **f**, Representative image of immunostaining of S100 (green) and Nefh (red) in circumferential fibres (arrowheads) and lanceolate endings (arrows) in the hair follicle of *Piezo2*^{WT} (**b**) and *Piezo2*^{CKO} dorsal skin (**e** and **f**). **c**, **g**, Representative image of immunostaining of S100 (green) and Nefh (red) in Meissner's corpuscles in *Piezo2*^{WT} (**c**) and *Piezo2*^{CKO} (**g**) glabrous skin. Bg, bulge of the hair follicle; Der, dermis; Epi, epidermis; HS, hair shaft. Scale bars, 20 μm.

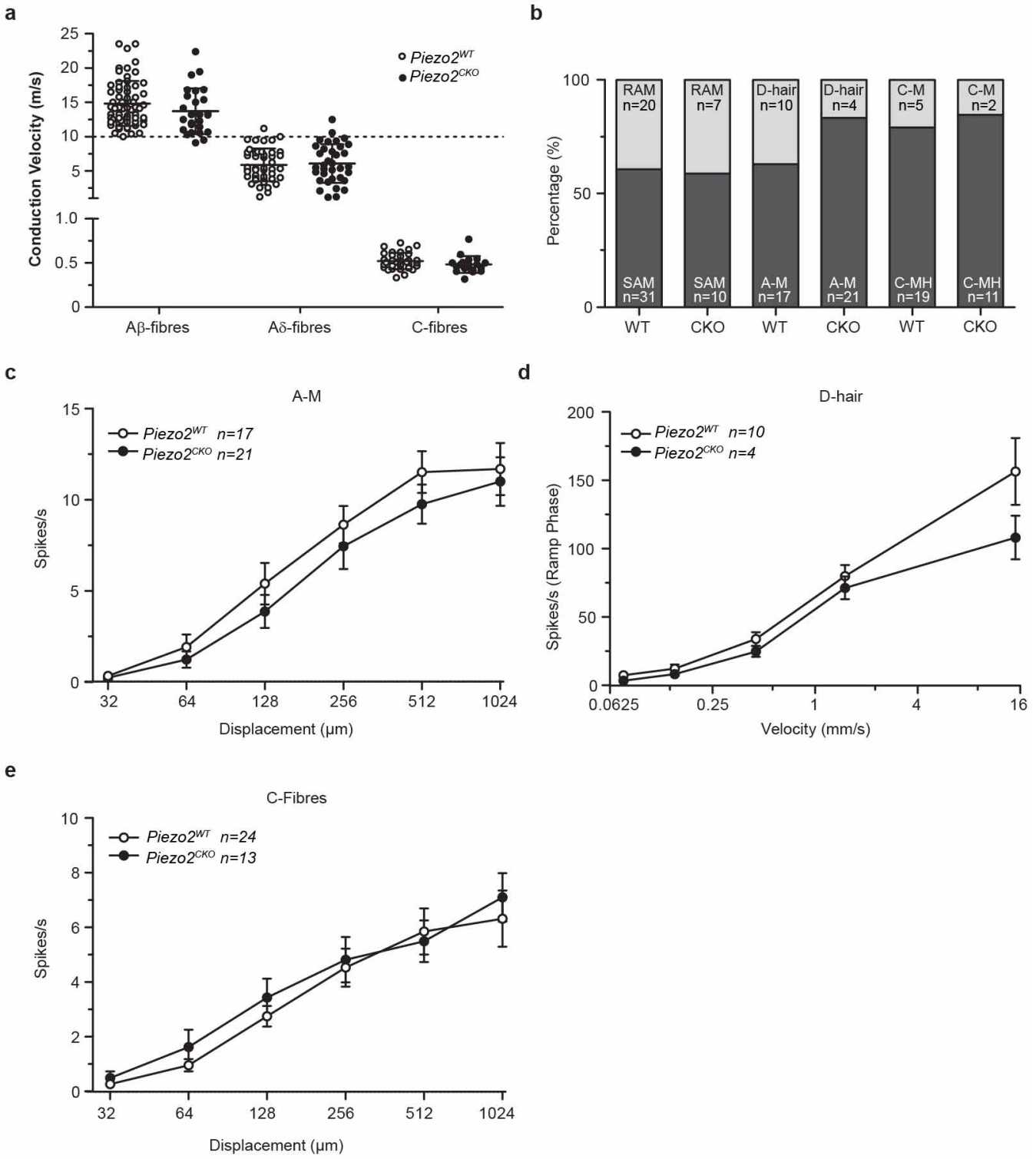

Extended Data Figure 5 | Physiological properties of nociceptors are unaffected in *Piezo2*^{CKO} mice. **a**, No change in conduction velocities of Aβ-, Aδ- and C-fibre afferents in *Piezo2*^{CKO} compared to *Piezo2*^{WT} (Mann–Whitney test). **b**, Proportions of receptor types encountered among Aβ, Aδ and C fibres are shown. A-M, Aδ mechanonociceptor; C-M, C mechanonociceptor; C-MH, C mechano/heat receptor, responding both to noxious heat and mechanical stimuli; RAM, rapidly adapting mechanoreceptor; SAM, slowly adapting mechanoreceptor. **c**, Stimulus response properties of Aδ mechanonociceptors recorded in *Piezo2*^{CKO} compared to *Piezo2*^{WT} were not significantly different. **d**, D-hair receptors recorded from *Piezo2*^{CKO} displayed stimulus response properties that were indistinguishable from control afferents. **e**, The stimulus response properties of C fibres in *Piezo2*^{CKO} were not significantly different from C fibres recorded in control *Piezo2*^{WT} mice. Data are presented as mean ± s.e.m., repeated measures ANOVA analysis for **c**–**e**.

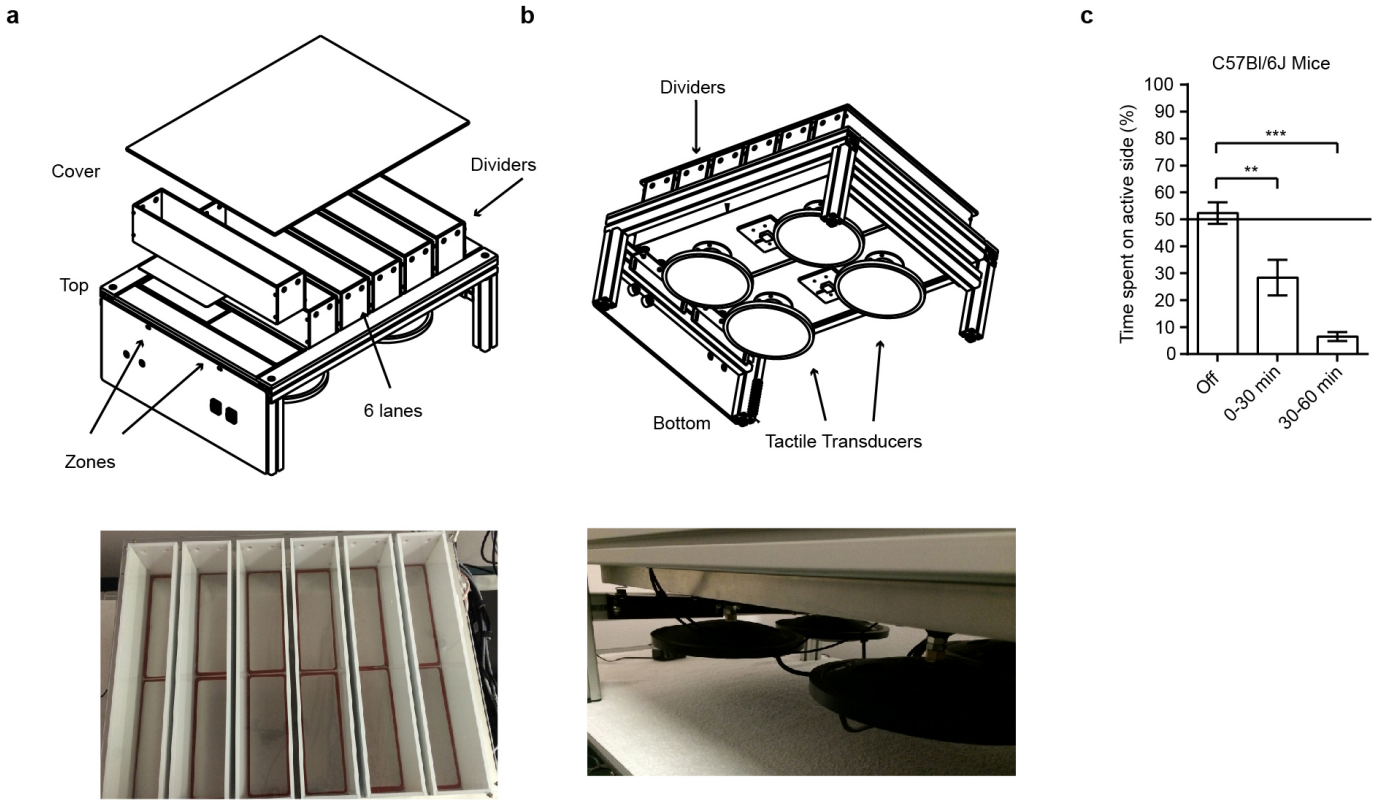

Extended Data Figure 6 | Development of the novel two-choice mechanosensory assay. **a**, Schematic of instrument construction and image of instrument from above. **b**, Schematic of the instrument from below, with the top cover removed, and photo of tactile transducers underneath the platform. **c**, Avoidance behaviour of C57BL/6J mice to the mechanically active side. Error bars represent s.e.m., $n = 12$ mice, 6 males and 6 females. $^{**}P < 0.005$, $^{***}P < 0.0001$, Mann–Whitney non-parametric analysis.

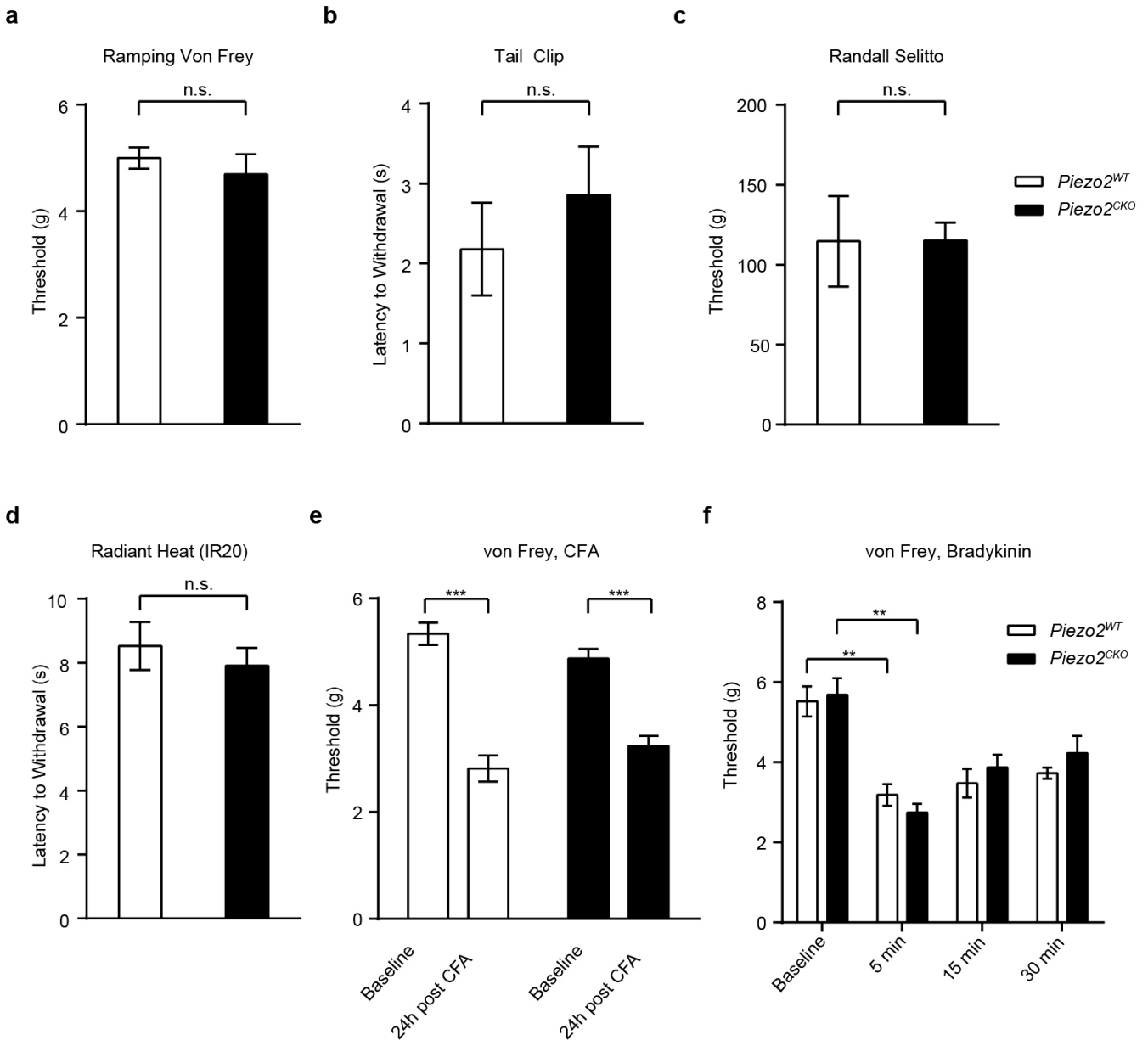

Extended Data Figure 7 | *Piezo2*^{CKO} mice do not show deficits in noxious mechanical or thermal stimuli or in inflammatory pain responses. **a**, Threshold for withdrawal response to a ramping protocol of von Frey stimulation from low force to high in *Piezo2*^{WT} ($n = 9$) and *Piezo2*^{CKO} ($n = 7$) mice. **b**, Time to response (latency) to application of a 500 g tail clip to the base of the tail in *Piezo2*^{WT} ($n = 6$) and *Piezo2*^{CKO} ($n = 7$) mice. **c**, Threshold for response to a Randall–Selitto pinching stimulus to the hind paw in *Piezo2*^{WT} ($n = 5$) and *Piezo2*^{CKO} ($n = 7$) mice. **d**, Time to withdrawal of hind paw in response to an infrared light heat source (Hargreaves assay) in *Piezo2*^{WT} ($n = 13$) and *Piezo2*^{CKO} ($n = 9$) mice. **e**, Ramping von Frey protocol in baseline (before CFA injection) and 24 h post CFA injection in *Piezo2*^{WT} ($n = 11$) and *Piezo2*^{CKO} ($n = 9$) mice. **f**, Ramping von Frey protocol in baseline (before bradykinin injection) and at time points 5, 15 and 30 min post injection in *Piezo2*^{WT} ($n = 6$) and *Piezo2*^{CKO} ($n = 6$) mice. Error bars represent s.e.m., all experiments performed with at least two separate cohorts of both male and female mice, $^{**}P < 0.005$, $^{***}P < 0.0001$, Mann–Whitney non-parametric analysis.

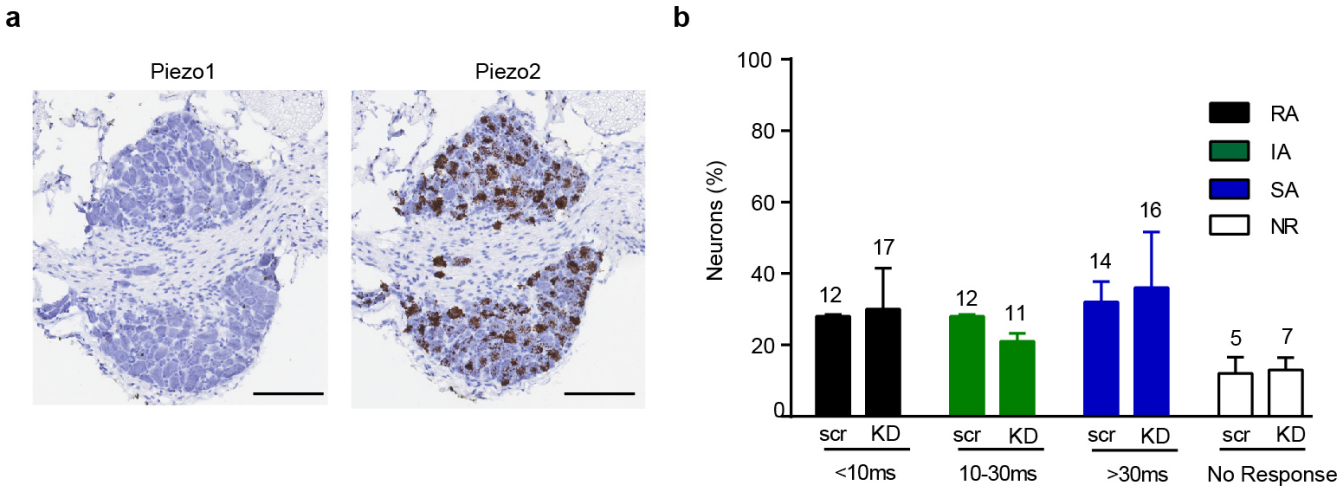

Extended Data Figure 8 | Piezo1 expression and function in DRGs. a, *In situ* hybridization expression analysis of Piezo1 in DRG neurons relative to Piezo2. Robust expression of Piezo2 but not Piezo1 is observed, and this agrees with previously reported results using qPCR[3]. **b**, siRNA for Piezo1 in cultured DRG neurons does not affect the number of mechanically sensitive neurons or the ratio of rapidly, intermediately or slowly adapting currents (number of recorded neurons in each category indicated on top of bar graphs). Data from three independent preparations, not significant by Student's *t*-test. Scale bar, 100 µm. KD, knockdown; scr, scrambled.

Extended Data Table 1 | Electrical properties of *Piezo2*^{WT} and *Piezo2*^{CKO} cultured DRG neurons

Properties	*Piezo2*^{WT}	*Piezo2*^{CKO}
Membrane Resistance (MΩ)	985 ± 140 (n=57)	860 ± 110 (n=62)
Access resistance, R_a (MΩ)	12.3 ± 0.5 (n=62)	12.7 ± 0.6 (n=57)
Holding current at -80mV (pA)	-272 ± 42 (n=57)	-235 ± 34 (n=62)
Resting membrane potential (mV)	-49.3 ± 0.9 (n=57)	-47.8 ± 1.1 (n=62)
Rheobase (pA)	430 ± 90 (57)	220 ± 35 (60)*
Number of AP at 2x rheobase	1.2 ± 0.1 (54)	1.2 ± 0.1 (59)
APD (msec)	2.45 ± 0.18 (57)	2.49 ± 0.15 (61)
APD range	0.4, 6	0.6, 5.2
AP overshoot (mV)	71.9 ± 1.6 (57)	70.7 ± 1.6 (61)

Values are mean ± s.e.m. (number of neurons). APD, action potential duration; AP, action potential; *$P < 0.05$, Student's *t*-test; rheobase values are not significantly different ($P=0.3$) when cells with many processes are removed from the data set (high rheobase, $n=7$ and 6 for *Piezo2*^{WT} and *Piezo2*^{CKO}, respectively).

Extended Data Table 2 | Properties of single fibres recorded from *Piezo2*^{WT} and *Piezo2*^{CKO} using the saphenous nerve *ex vivo* skin nerve preparation

a

Subclass		*Piezo2*^{WT}	*Piezo2*^{CKO}
Aβ-fibres	SAM I	22	7
	SAM II	9	3
	RAM	20	7
Aδ-fibres	D-Hair	10	4
	A-M	17	21
C-fibres	C-LT	-	-
	C-M	5	2
	C-MH	15	8
	C-MHC	4	3

b

	Piezo2^{WT}	*Piezo2*^{CKO}
Mechanically Sensitive	84	58
Mechanically Insensitive	4	13

a, Mechanical search protocol. **b,** Electrical search protocol. C-LT, C fibre with low-threshold mechanosensitivity; C-M, C mechanonociceptor only responding to mechanical stimulation and not noxious cold or heat; C-MH, C mechano/heat receptor, responding both to noxious heat and mechanical stimuli; C-MHC, C mechano/heat/cold fibre responding to noxious mechanical, hot and cold stimulation; SAM II, slowly adapting mechanoreceptor type II. Note that small discrepancies between the numbers of fibres listed here and those tested with the full series of mechanical stimuli are due to technical issues preventing full characterization of the unit.